



Modelling and design of a perfectly-absorbing wave energy converter

R. Porter

School of Mathematics, Fry Building, Woodland Road, University of Bristol, Bristol, BS8 1UG, UK.

Abstract

This paper concerns the absorption of energy from two-dimensional water waves propagating over fluid of constant depth by a wave energy converter consisting of small buoyant floating rafts constrained to move in heave motion and attached to the bed with springs and dampers. Under a shallow water approximation to the fluid motion, it is shown that spatially-varying spring and damper settings allow all of the wave energy to be absorbed from all wave frequencies. The basis of the design is a formulation of a novel type of ‘Perfectly Matched Layer’ equation which can be mapped onto a shallow water model of the wave energy converter. The theoretical predictions are tested with computations based on a full description of linearised water waves and show that near-perfect absorption persists over a wide range of wave frequencies.

Keywords: Wave energy converter, perfectly matched layer, complete absorption.

1. Introduction

1 This paper concerns the absorption of energy from two-dimensional water waves incident on
2 an array of buoys floating on the surface of a fluid. The question we concern ourselves with is
3 whether it is possible to design the operation of these buoys to absorb all of the available incoming
4 wave energy, not just at a single frequency but across wave frequencies. There is well-established
5 theory (e.g. Evans (1976)) and multiple examples of two-dimensional ocean wave energy ab-
6 sorbers capable of extracting 100% of the wave energy, but only at particular wave frequencies.
7 Examples include Salter’s Duck (Salter (1974), Salter *et al.* (1976)) and the Bristol Cylinder
8 (Evans *et al.* (1979)).

9 Our question will be addressed within the framework of linearised shallow water theory in
10 which it is assumed the wavelength of propagating waves is significantly larger than the depth.
11 Waves are incident from $x < 0$ over constant depth and the absorbing array of floating buoys
12 extend into $x > 0$. The buoys are assumed to be much smaller in width than the wavelength
13 and are connected to the bottom of the fluid by springs and dampers. The spring and damper
14

Email address: richard.porter@bristol.ac.uk (R. Porter)

15 settings are allowed to vary spatially along the device. We will show that it is possible under this
 16 framework to achieve perfect absorption across all frequencies.

17 The study in this paper is of more theoretical than practical interest. First, shallow water theory
 18 is an approximation for $kh \ll 1$ which is only exact (e.g. Porter (2019)) in the limit of $kh \rightarrow 0$
 19 (k being the wavenumber, h the depth) and wave energy converters would be expected to operate
 20 in the regime $kh = O(1)$. Second, the perfectly-absorbing wave energy converter design extends
 21 indefinitely into $x > 0$ and requires a short initial segment of the array to contain negative dampers.
 22 On the other hand, the particular design being proposed within this paper does have some close
 23 relatives that have been considered as practical wave absorbers in the form of floating articulated
 24 rafts of the type originally conceived by Cockerell *et al.* (1978) and subsequently studied theo-
 25 retically and numerically by Haren & Mei (1979) and Newman (1979). Significantly, the work
 26 of Haren & Mei (1979) was performed using shallow water assumptions and they carried out a
 27 comparison with numerical results for arbitrary depth suggesting that shallow water predictions
 28 performed well for larger fluid depths.

29 Compact arrays of floating buoys moving independently in heave as wave energy absorbers
 30 have been studied recently by Garnaud & Mei (2009) though not under shallow water theory.
 31 Garnaud & Mei (2009) use a multi-scale homogenisation method to develop an effective boundary
 32 condition to take account of the presence of the buoys based on their horizontal lengthscale being
 33 much smaller than that of the wavelength and their draft being insignificant. This careful approach
 34 is equivalent to invoking a continuum description of the surface loading similar to that proposed
 35 by Weitz & Keller (1950) and is how we choose to present the modelling here.

36 The paper contains two novel elements. The first is the development of a model of compact
 37 arrays of absorbing buoys under shallow water assumptions (see Section 4). This model has been
 38 derived in a physically intuitive manner although careful asymptotic analysis is needed to establish
 39 the correct matching conditions at the junction between the device and open water. The second
 40 is the development of a new family of equations which can be perfectly impedance matched at
 41 the boundary $x = 0$ between the unloaded and loaded surfaces and gives rise to wave decay in
 42 $x > 0$ (see Section 3.1). These ideas are related to the Perfectly Matched Layer (PML) equations
 43 originally due to Berenger (1994) which are explained, for context, in Section 3 of the paper. In
 44 Section 5 we consider the full linearised equations of water waves and produce numerical results
 45 to test the design of the proposed wave energy converter over a range of frequencies beyond
 46 $kh \ll 1$ and into $kh = O(1)$. We also assess the effect that the length of truncated devices have on
 47 absorption efficiency. The paper is summarised in Section 6.

48 2. Linearised shallow water equations

49 This short section provides an outline derivation of the linearised shallow water equation – see
 50 e.g. Stoker (1957) or Mei (1983) and references therein. It provides a platform for later discussion
 51 and model derivation.

52 Cartesian coordinates (x, z) are used with x lying horizontally in, and z upwards from, the
 53 mean free surface of a fluid of density ρ and constant depth h subject to gravity, g . The flow
 54 is two-dimensional with velocity $\mathbf{u} = U\hat{\mathbf{x}} + W\hat{\mathbf{z}}$ and support waves of height $\zeta(x, t)$. Shallow
 55 water assumes that the characteristic wavelength L is much greater than the depth and implies that

56 $U = U(x, t)$ and $W \ll U$ to leading order in h/L . Integrating $\nabla \cdot \mathbf{u} = 0$ with respect to z over the
57 fluid depth, using the kinematic condition $\zeta_t = W$ on $z = \zeta$, gives

$$\zeta_t = -(h + \zeta)U_x \approx -hU_x \quad (1)$$

58 (i.e. equations are linearised supposing waves of sufficiently small amplitude). The z -component
59 of the linearised Euler equations is approximately (i.e. neglecting W_t , a consequence of the shallow
60 water assumption) $p_z = -\rho g$ and integrating, using $p = p_a$ (constant atmospheric pressure) on
61 $z = \zeta$, gives

$$p = p_a + \rho g(\zeta - z). \quad (2)$$

62 The x -component of the linearised Euler equations is $\rho U_t = -p_x$ which then gives

$$U_t = -g\zeta_x \quad (3)$$

63 and combining equations to eliminate U gives

$$\zeta_{tt} = c^2 \zeta_{xx} \quad (4)$$

64 where $c = \sqrt{gh}$.

65 3. Perfectly Matched Layers

66 Berenger's (1994) paper describes a method for absorbing waves at the boundary of trun-
67 cated domains, designed for use in numerical methods aimed at providing computational so-
68 lutions to solve Maxwell's equations. In his paper Berenger considered two-dimensional time-
69 dependent problems associated with transverse electric/magnetic polarised waves and prescribed
70 a non-physical set of partial differential equations (PDEs) which are perfectly impedance-matched
71 to Maxwell's equations. These provide a reflectionless boundary across which obliquely-incident
72 wave energy is perfectly transmitted and then progressively damped. Although the original method
73 has been developed, generalised and adapted to other field theories, Berenger's original work
74 considered Maxwell's equations under polarisation as coupled first-order PDEs for the electric
75 and magnetic fields. The so-called Perfectly Matched Layer (PML) equations involve addition
76 of damping to each equation in exactly the right balance to match the impedance to that of free
77 space. For our purposes we consider how the PML works in a simpler one-dimensional setting and
78 relating to waves on shallow water described, as already shown, by two field variables satisfying
79 coupled first-order PDEs.

80 In $x < 0$ we take the shallow water equations (1), (3) or combined as (4). In $x > 0$ the PML is
81 defined by the non-physical equations

$$U_t + c\lambda U = -g\zeta_x, \quad \zeta_t + c\lambda\zeta = -hU_x \quad (5)$$

82 where λ is a positive constant, which may also be combined to give

$$\zeta_{tt} + 2c\lambda\zeta_t + c^2\lambda^2\zeta = c^2\zeta_{xx}. \quad (6)$$

83 The matching conditions at $x = 0$ are that ζ is continuous (a proxy for pressure) and U is continu-
 84 ous (mass flux). To see how the PML works we write $\zeta = \Re\{\eta(x)e^{-i\omega t}\}$, $U(x, t) = \Re\{u(x)e^{-i\omega t}\}$ so
 85 that the equations (4) and (6) in the frequency domain are

$$\eta''(x) + k^2\eta(x) = 0, \quad x < 0 \quad (7)$$

86 where $k = \omega/c$ and

$$\eta''(x) + (k^2 + 2ik\lambda - \lambda^2)\eta(x) = 0, \quad x > 0 \quad (8)$$

87 with the matching conditions in the frequency domain found to be

$$\eta(0^-) = \eta(0^+), \quad \eta'(0^-) = \frac{k}{k + i\lambda}\eta'(0^+). \quad (9)$$

88 Solutions of (7) due to an incident wave from minus infinity are given by $\eta = e^{ikx} + Re^{-ikx}$ where R
 89 is the reflection coefficient whilst solutions of (8) are $\eta = Te^{i(k+i\lambda)x}$ with the transmission coefficient
 90 T associated with outgoing waves which decay as $x \rightarrow \infty$. The matching conditions (9) determine
 91 that $R = 0$ and $T = 1$. Since λ is a constant independent of frequency it follows that waves of
 92 all frequencies incident from $x < 0$ are absorbed without reflection by the PML equations (6) in
 93 $x > 0$.

94 It is hard to map the PML equations (5) onto a model of a physical system. Of particular
 95 difficulty is the conservation of mass equation which is modified in the second equation in (5) to
 96 include loss.

97 The PML of Berenger was modified and extended to a Generalised PML (GPML) by Fang
 98 & Zu (1995) to overcome some of the shortcomings of the PML, including its deficiency in sup-
 99 pressing evanescent waves. The downside of the GPML is that it is designed to operate for single
 100 frequency wave motion in which (5) become

$$(-i\omega + c\lambda(x))u = -g\eta', \quad (-i\omega + c\lambda(x))\eta = -hu'. \quad (10)$$

101 In return, λ is no longer required to be constant and the two equations above combine to give

$$-\frac{\omega^2}{c^2}\eta = \frac{1}{1 + i\lambda(x)c/\omega} \left(\frac{\eta'}{1 + i\lambda(x)c/\omega} \right)'. \quad (11)$$

102 These equations result from what is sometimes referred to as ‘coordinate stretching’ of the un-
 103 damped wave equation (4) via the complex mapping $x \rightarrow x + (ic/\omega) \int^x \lambda(s) ds$ and results in
 104 solutions in $x > 0$ of the form

$$\eta = T \exp \left\{ ikx - \int^x \lambda(s) ds \right\}. \quad (12)$$

105 When λ is a constant we recover the Berenger PML, but this framework allows for the attenuation
 106 rate to increase smoothly which is important when implemented in discrete computational schemes
 107 like finite differences in suppressing numerically-induced reflections.

108 The time-domain PDE associated with (11), used in finite-difference time-domain numerical
 109 schemes, is

$$\frac{1}{c^2} \zeta_{tt} = \frac{1}{1 + i\lambda(x)c/\omega} \frac{\partial}{\partial x} \left(\frac{1}{1 + i\lambda(x)c/\omega} \frac{\partial \zeta}{\partial x} \right) \quad (13)$$

110 and, as already stated, there is an assumed frequency ω built into this PDE implying perfect ab-
 111 sorption is tuned only to a particular frequency. There are extensions which incorporate frequency-
 112 independent PMLs but these add a significant degree of complication to the method which is not
 113 needed for the purposes of this paper.

114 3.1. A different approach

115 In $x < 0$ consider, as before, the one-dimensional frequency-domain wave equation

$$\eta''(x) + k^2 \eta(x) = 0 \quad (14)$$

116 where $k > 0$ is constant and in $x > 0$ let η be governed by a general equation

$$\eta''(x) + \kappa(x)\eta(x) = 0 \quad (15)$$

117 and matching conditions at $x = 0$ are posed as

$$\eta(0^+) - \eta(0^-) = \beta \eta'(0^-), \quad \eta'(0^+) = \alpha \eta'(0^-) \quad (16)$$

118 where α, β are constants. For the application we have in mind α, β will be real positive constants,
 119 independent of k , which puts our problem beyond the scope of the PML methods previously dis-
 120 cussed.

121 We want to determine possible functions $\kappa(x)$ such that all incoming waves from $x = -\infty$ are
 122 absorbed in $x > 0$ and nothing is reflected by the boundary at $x = 0$.

123 In $x < 0$ the general solution of (14) is once again

$$\eta(x) = e^{ikx} + R e^{-ikx} \quad (17)$$

124 and so $\eta(0^-) = (1 + R)$ and $\eta'(0^-) = ik(1 - R)$. In $x > 0$ we impose a solution of the form

$$\eta(x) = T e^{iAkx - f(x)} \quad (18)$$

125 where A is a positive real constant such that $f(0) = 0$ and $f(x)$ is a positive increasing function of
 126 x as $x \rightarrow \infty$ in order that $\eta(x) \rightarrow 0$ at infinity.

127 It follows that $\eta(0^+) = T$ and $\eta'(0^+) = (iAk - f'(0))T$ and application of the matching conditions
 128 (16) gives

$$T - R - 1 = ik\beta(1 - R), \quad (iAk - f'(0))T = ik\alpha(1 - R). \quad (19)$$

129 Setting the reflection coefficient to zero, $R = 0$, gives $T = 1 + i\beta k$ with

$$A = \frac{\alpha}{1 + \beta^2 k^2}, \quad f'(0) = \frac{-\beta k^2 \alpha}{1 + \beta^2 k^2}. \quad (20)$$

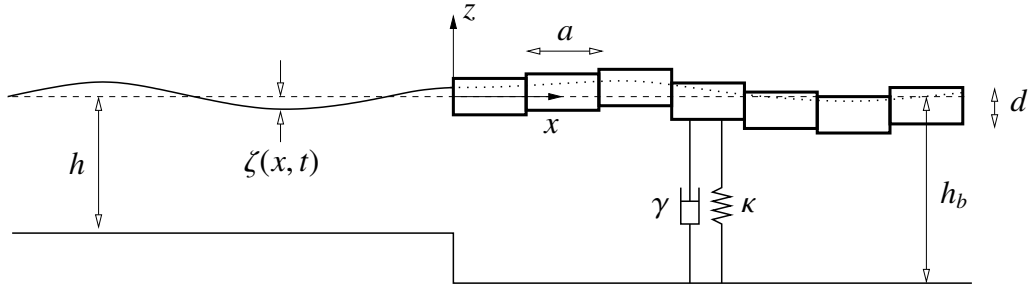


Figure 1. Sketch of the discrete floating absorbers and definition of the geometry.

130 as conditions on A and the function $f(x)$ for total absorption. From the definition (18) in $x > 0$

$$\eta'(x) = (iAk - f'(x))\eta(x) \quad (21)$$

131 and then

$$\eta''(x) = -f''(x)\eta(x) + (iAk - f'(x))^2\eta(x). \quad (22)$$

132 Comparison with (15) shows that

$$\kappa(x) = A^2k^2 + f''(x) - f'^2(x) + 2iAkf'(x). \quad (23)$$

133 Note that if $\alpha = 1 + i\lambda/k$, $\beta = 0$ and $f(x) = 0$ then we exactly recover the PML equations.

134 4. Shallow water model for an array of floating absorbers

135 Imagine that $x < 0$ an uncovered fluid is of constant depth h such that (4) holds and in $x > 0$
 136 small buoyant rafts form a continuous cover of the surface of the fluid, each raft constrained to
 137 move in heave independently of its neighbours (see Fig. 1). The density of the buoys is $\rho_b < \rho$ and
 138 their depth is d so the draft of the buoys at rest is $\hat{\rho}d$ where $\hat{\rho} = \rho_b/\rho$. The width of the buoys, a
 139 say, is assumed to be much smaller than the wavelength and consequently the vertical displacement
 140 from equilibrium of the buoys due to the fluid motion may be described by a continuous function
 141 $\zeta(x, t)$ which satisfies the following dynamic equation

$$\rho_b d \zeta_{tt} = p|_{z=-\hat{\rho}d+\zeta} - p_a - \rho_b d g - \gamma \zeta_t - \sigma \zeta. \quad (24)$$

142 Each buoy is attached to a linear damper, γ , and a spring of spring constant σ (attributed values
 143 are per unit length). All terms in this equation can be varying slowly (on a lengthscale no smaller
 144 than that of the wavelength) with x under this continuum description of the buoys. This continuum
 145 description can be justified formally using multi-scale homogenisation similar to Garnaud & Mei
 146 (2009). Vertically integrating the continuity equation through the fluid $-h_b < z < -\hat{\rho}d + \zeta$ where
 147 h_b is the fluid depth under the buoys gives rise to

$$\zeta_t = -(h_b - \hat{\rho}d)U_x \quad (25)$$

148 after linearisation whilst vertical momentum integrates to $p = P(x, t) - \rho g z$ as before which, when
 149 used in (24) above, determines that

$$P(x, t) = \rho_b d \zeta_{tt} + p_a + \gamma \zeta_t + \sigma \zeta + \rho g \zeta. \quad (26)$$

150 Thus

$$p = p_a + \rho g (\zeta - z) + \rho_b d \zeta_{tt} + \gamma \zeta_t + \sigma \zeta \quad (27)$$

151 is the pressure in the fluid which, when used in horizontal momentum, $\rho U_t = -p_x$, gives

$$U_t = -g \zeta_x - \partial_x (\hat{\rho} d \zeta_{tt} + (\gamma/\rho) \zeta_t + (\sigma/\rho) \zeta). \quad (28)$$

152 Eliminating U between (25) and (28) results in the governing equation

$$\zeta_{tt} = (h_b - \hat{\rho} d) g \zeta_{xx} + (h_b - \hat{\rho} d) \partial_{xx} (\hat{\rho} d \zeta_{tt} + (\gamma/\rho) \zeta_t + (\sigma/\rho) \zeta) \quad (29)$$

153 under shallow water assumptions for wave propagation through floating buoys.

154 The matching conditions at $x = 0$ are that the pressure and mass flux are continuous. The
 155 second of these implies $hU(0^-, t) = (h_b - \hat{\rho} d)U(0^+, t)$ and results in

$$\frac{h}{h_b - \hat{\rho} d} \zeta_x(0^-, t) = \zeta_x(0^+, t) + \partial_x ((\hat{\rho} d/g) \zeta_{tt} + (\gamma/\rho g) \zeta_t + (\sigma/\rho g) \zeta)|_{x=0^+}. \quad (30)$$

156 The first condition requires rather more careful attention. Shallow water theory is derived under
 157 the assumption that $\epsilon = kh = \omega \sqrt{h/g} \ll 1$ and subsequently expanding field variables in powers
 158 of ϵ . We have chosen to spare the reader that level of detail in order to preserve a more physical
 159 approach to the model derivation. However, we cannot completely ignore the consequences of
 160 a more formal approach which produce a boundary condition which is not physically intuitive.
 161 Thus, equations presented in this paper describing the fluid motion include contributions from
 162 zeroth and first order problems. In particular the damping term, which is associated with a time
 163 derivative, only enters the equations for the absorber in $x > 0$ at $O(\epsilon)$ and this is an effect which
 164 we are required to capture. We remark that expanding further to $O(\epsilon^2)$ is a far more serious
 165 undertaking (see Porter (2019)) and not one we need to entertain here. However, had it only been
 166 necessary to expand to zeroth order in ϵ then our matching condition would be that the pressure
 167 as $x \rightarrow 0^-$ matches the pressure as $x \rightarrow 0^+$ (this principle was applied to arrive at the first relation
 168 in (9)). The reason this is not an obvious condition to apply at higher orders is due to the abrupt
 169 change to the geometry at $x = 0$ in the levels of both the upper and lower fluid boundaries (see
 170 Fig. 1). This change to the vertical structure of the fluid implies that the shallow water models
 171 do not apply in the vicinity of $x = 0$. Formally, the matching across $x = 0$ from the solution in
 172 $x < 0$ to the solution in $x > 0$ must be performed by asymptotic matching to the solution of an
 173 inner problem with coordinates scaled to the depth, much smaller than the wavelength scale. This
 174 process contributes to the pressure matching condition at $O(\epsilon)$ and relating the pressure jump to the
 175 upstream flux multiplied by a “blockage coefficient” which depends only on the local geometry.
 176 This coefficient is found by solving a potential flow problem through the junction at $x = 0$ on which
 177 all lateral boundaries have Neumann conditions imposed and subject to unit upstream volume flux
 178 (see Appendix).

179 Such a process is described in excellent detail by Mei (1983), following Tuck (1975), for the
 180 problem of surface wave propagation over a step in the bed under shallow water conditions. In that
 181 work it is shown that changes in the modulus of the reflection coefficient due to the inclusion of a
 182 blockage coefficient appear at $O(\epsilon^2)$ which justifies their neglect. Here, unfortunately, the effect of
 183 the blockage coefficient cannot be so easily overlooked although its final effect is rather small.

184 Thus the difference in dynamic pressure equates to $-\rho(hU(0^-, t)[\psi])_t$ where $[\psi] = B$ is the po-
 185 tential difference and equal to the positive real blockage coefficient, B , multiplied by the upstream
 186 flux and is written, using (2), (27) as the condition

$$\rho g \zeta(0^+, t) + \rho_b d \zeta_{tt}(0^+, t) + \gamma \zeta_t(0^+, t) + \sigma \zeta(0^+, t) - \rho g \zeta(0^-, t) = -\rho B h U_t(0^-, t) \quad (31)$$

187 simplifying to

$$\zeta(0^+, t) + (\hat{\rho}d/g)\zeta_{tt}(0^+, t) + (\gamma/\rho g)\zeta_t(0^+, t) + (\sigma/\rho g)\zeta(0^+, t) - \zeta(0^-, t) = B h \zeta_x(0^-, t) \quad (32)$$

188 after use of (3).

189 4.1. Frequency domain equations

190 In the case that waves of a single frequency, ω , are sought we write $\zeta(x, t) = \Re\{\eta(x)e^{-i\omega t}\}$ and
 191 $U(x, t) = \Re\{u(x)e^{-i\omega t}\}$ as before so that (4) becomes

$$\eta''(x) + k^2\eta(x) = 0, \quad x < 0 \quad (33)$$

192 with $k = \omega/c$ and (29) is

$$\left(\left(1 - k^2 \hat{\rho} d h - i k \frac{\gamma}{\rho} \sqrt{\frac{h}{g} + \frac{\sigma}{\rho g}} \right) \eta(x) \right)'' + \frac{k^2}{\hat{h}} \eta(x) = 0, \quad (34)$$

193 in $x > 0$ where $\hat{h} = (h_b - \hat{\rho}d)/h$. It helps to write $\hat{\sigma} = \sigma/\rho g$ and $\hat{\gamma} = \gamma/\rho \sqrt{gh}$ and, to be consistent
 194 with the derivation of the shallow water equation which implicitly neglect terms of order $O(kh)^2$,
 195 the equation above reads

$$((1 - i k h \hat{\gamma} + \hat{\sigma})\eta(x))'' + \frac{k^2}{\hat{h}} \eta(x) = 0. \quad (35)$$

196 We also make a change of variable

$$\tilde{\eta}(x) = (1 - i k h \hat{\gamma} + \hat{\sigma})\eta(x), \quad (36)$$

197 say, so that

$$\tilde{\eta}''(x) + \frac{k^2 \tilde{\eta}(x)}{\hat{h}(1 - i k h \hat{\gamma} + \hat{\sigma})} = 0 \quad (37)$$

198 and recall that $\hat{\sigma}$ and $\hat{\gamma}$ can be functions of x varying on the lengthscale $O(1/k)$. It is straightforward
 199 to determine that the matching conditions (32), (30) have become, under both the transformations
 200 into the frequency domain and under the change of variable (36),

$$\tilde{\eta}(0^+) - \eta(0^-) = B h \eta'(0^-) \quad (38)$$

201 and

$$\tilde{\eta}'(0^+) = \hat{h}^{-1}\eta'(0^-). \tag{39}$$

202 Using the shallow water assumption $kh \ll 1$ and, providing $\hat{\gamma} = O(1)$, we can approximate (37) by

$$\tilde{\eta}''(x) + \frac{k^2}{\hat{h}} \left(\frac{1}{1 + \hat{\sigma}} + ikh \frac{\hat{\gamma}}{(1 + \hat{\sigma}^2)} \right) \tilde{\eta}(x) = 0 \tag{40}$$

203 a process equivalent to a formal asymptotic expansion of the governing equations to $O(kh)$. This
 204 governing equation with the matching conditions (38), (39) are aligned to the general system
 205 described in §3.1.

206 *4.2. Perfect absorption*

207 With reference to §3.1 we let $\alpha = \hat{h}^{-1}$, $\beta = Bh$ and it follows from (20) that

$$A = \frac{1}{\hat{h}(1 + Bk^2h^2)} \approx \frac{1}{\hat{h}} \tag{41}$$

208 and

$$f'(0) = -\frac{Bk^2h}{\hat{h}(1 + Bk^2h^2)} \approx -Bk^2h/\hat{h} \tag{42}$$

209 after ignoring $O(kh)^2$ to be consistent with the shallow water assumption. We are free to choose
 210 any $f(x)$ provided (42) holds, $f(0) = 0$ and $f(x)$ is positive increasing function of x as $x \rightarrow \infty$. We
 211 make the choice, for δ a positive constant,

$$f(x) = \frac{k^2h^2}{\delta} \ln \cosh(\delta x/h) - k^2hBx/\hat{h} \tag{43}$$

212 with $B/\hat{h} < 1$ and $f(x) \sim k^2h(1 - B/\hat{h})x$ as $x \rightarrow \infty$. In making the particular choice (43) we have
 213 been mindful of the consequences for the modelling assumptions, in particular that $\hat{\gamma} = O(1)$ and
 214 that spring constants should be positive. It follows that (15) holds with

$$\kappa(x) = \frac{k^2}{\hat{h}} \left[\frac{1}{\hat{h}} + \hat{h}\delta(1 - \tanh^2(\delta x/h)) + \hat{h}k^2h^2(\tanh(\delta x/h) - B/\hat{h})^2 + 2ikh(\tanh(\delta x/h) - B/\hat{h}) \right]. \tag{44}$$

215 In view of wanting to align (44) with the coefficient in front of $\tilde{\eta}(x)$ in (40) we let \hat{h} satisfy $\hat{h}^{-1} + \delta\hat{h} =$
 216 1 to give

$$\hat{h} = (1 - \sqrt{1 - 4\delta})/(2\delta) \tag{45}$$

217 ($0 < \delta \leq \frac{1}{4}$) and $\hat{h} \approx 1 + \delta$ for $\delta \ll 1$. Neglecting the $O(kh)^2$ term to be consistent with the shallow
 218 water equation derivation we can equate (44) to

$$\kappa(x) = \frac{k^2}{\hat{h}} \left(\frac{1}{1 + \hat{\sigma}} + ikh \frac{\hat{\gamma}}{(1 + \hat{\sigma}^2)} \right) \tag{46}$$

219 with

$$\hat{\sigma}(x) = \frac{\delta\hat{h} \tanh^2(\delta x/h)}{1 - \delta\hat{h} \tanh^2(\delta x/h)}, \quad \hat{\gamma}(x) = \frac{2(\tanh(\delta x/h) - B/\hat{h})}{(1 - \delta\hat{h} \tanh^2(\delta x/h))^2} \tag{47}$$

220 such that $\hat{\sigma}(x)$ increases monotonically from 0 at the origin to $\delta\hat{h}/(1 - \delta\hat{h})$ at infinity. The damper
 221 settings are positive (absorbing) for $x > (h/\delta) \tanh^{-1}(B/\hat{h})$ and tend to the value $2(1 - B/\hat{h})/(1 - \delta\hat{h})^2$
 222 as $x \rightarrow \infty$. However, for $0 < x < (h/\delta) \tanh^{-1}(B/\hat{h})$ the dampers are negative and consume energy
 223 to drive the device. The important feature of the springs and dampers in (47) is that they are
 224 independent of frequency and so this physical system absorbs all of the wave energy from all
 225 frequencies (albeit within the bounds of the model, namely shallow water).

226 The rate at which waves are damped is frequency dependent, since, for $kx \gg 1$

$$\eta \approx (1 + ikhB) \exp\{ikx/\hat{h} - k^2h(1 - B/\hat{h})x\} \quad (48)$$

227 far into the array of absorbers, independent of the choice of δ . From a practical perspective, it
 228 would mean the array of floating absorbers would have to extend a distance in excess of $1/(k^2h)$ to
 229 get close to absorbing all of the available energy.

230 The value of B depends upon the local geometry – see the Appendix for the specification of the
 231 problem which determines B . If δ is small then $\hat{h} = 1 + \delta$ and the downstream fluid width is only
 232 marginally larger than upstream. If the draft of the buoys $\hat{\rho}d \ll h$ is small then the local junction
 233 in the geometry at $x = 0$ has little effect on the streaming flow and $B/\hat{h} \ll 1$. For example, for
 234 the shallow draft approximation given in (64) of the Appendix, $B/\hat{h} \approx -\delta^2 \ln(\delta/2)/\pi$ for $\delta \ll 1$
 235 and the length of the interval of the array which requires negative dampers is small relative to the
 236 depth: approximately $-\delta h \ln(\delta/2)/\pi$.

237 There may be other ways of representing wave attenuation through the buoy array with a choice
 238 of $f(x)$ different (43), which provide alternative solutions to the one proposed here.

239 5. Full linear theory

240 A question of immediate attention is whether the shallow water model developed in the previ-
 241 ous section for the design of a perfect all-frequency wave energy converter extends beyond $kh \ll 1$
 242 to $kh = O(1)$, a more practical range of frequencies. To answer this we must consider the full lin-
 243 earised equations for the small amplitude motion of a fluid with a free surface. In $x < 0$ where
 244 the surface is unloaded and the depth of the fluid is h , the fluid motion is governed by a velocity
 245 potential $\Phi(x, z, t)$ satisfying

$$\nabla^2 \Phi = 0 \quad (49)$$

246 over $-h < z < 0$ with

$$g\Phi_z + \Phi_{tt} = 0, \quad \text{on } z = 0 \quad \text{and} \quad \Phi_z = 0, \quad \text{on } z = -h. \quad (50)$$

247 In $x > 0$ the surface is covered with a compact array of independent heaving shallow-drafted
 248 floating buoys connected to springs and dampers over a bed of depth h_b . The governing Laplace
 249 equation (49) still holds for $-h_b < z < -\hat{\rho}d$ with $\Phi_z = 0$ on $z = -h_b$. On $z = -\hat{\rho}d$ the kinematic
 250 boundary condition is $\Phi_z = \zeta_t$ whilst the dynamic condition remains as (24), reliant on the con-
 251 tinued assumption that the width, a , of each buoy is significantly smaller than the wavelength, but
 252 with the pressure in the fluid given by linearised Bernoulli's equation as

$$p = p_a - \rho\Phi_t - \rho g(-\hat{\rho}d + \zeta(x, t)). \quad (51)$$

253 The result of combining dynamic and kinematic conditions is

$$g \left(1 + \frac{\hat{\rho}d}{g} \partial_{tt} + \frac{\gamma}{\rho g} \partial_t + \frac{\sigma}{\rho g} \right) \Phi_z + \Phi_{tt} = 0, \quad z = -\hat{\rho}d. \quad (52)$$

254 Writing $\Phi(x, z, t) = \Re\{\phi(x, z)e^{-i\omega t}\}$ implies $\nabla^2 \phi = 0$ in the fluid and $\phi_z = 0$ on the bed of the fluid
255 whilst from (50) and (51) we have

$$\phi_z - (\omega^2/g)\phi = 0, \quad z = 0, \quad x < 0 \quad (53)$$

256 and

$$\phi_z - F(x)\phi = 0, \quad z = -\hat{\rho}d, \quad x > 0 \quad (54)$$

257 where

$$F(x) = \frac{(\omega^2/g)}{1 - \omega^2 \hat{\rho}d/g - i(\omega \sqrt{h/g})\hat{\gamma}(x) + \hat{\sigma}(x)} \quad (55)$$

258 after using the same scalings on γ and σ introduced after (34).

259 This last boundary condition coincides with the one derived by Garnaud & Mei (2009) in a
260 more general setting where buoys of circular cross section cover a fractional area of the surface,
261 after taking into account the additional spring term. The total surface cover assumed here implies
262 the inertia term proportional to ω^2 in the denominator, discarded at leading order by Garnaud &
263 Mei (2009) on account of their scaling arguments, should be retained here. An independent study
264 (by the current author, in preparation) confirms this. On the other hand the ratio of d/h is likely
265 to be small and its effect is likely to be insignificant. Although Garnaud & Mei (2009) considered
266 only constant damping, implicit in the multi-scale method used in the derivation of (52) is the
267 capacity for the dampers $\hat{\gamma}$ and $\hat{\sigma}$ to vary on the lengthscale of the wavelength.

268 The task, therefore, is to design $\hat{\gamma}(x)$, $\hat{\sigma}(x)$ and select h_b to manufacture the same effect as in
269 shallow water, namely total absorption of incoming wave energy over all frequencies. Evidently,
270 the difficulty of this task is much increased here.

271 Instead, we take a different route and consider whether the perfect absorber design of $\hat{\gamma}(x)$, $\hat{\sigma}(x)$
272 made under shallow water conditions $kh \ll 1$ (equations (47)) work well for larger frequencies.

273 5.1. A ‘mild slope’ approach

274 Rather than attempt to solve the full linear equations directly we appeal to the fact that δ is
275 small and the coefficient in surface condition (55) with (47) varies slowly with x/h . Because
276 of this, we can use the approximation of Porter & Porter (2006) designed originally for solving
277 two-dimensional wave scattering by significant changes in bathymetry. In that paper a conformal
278 mapping of the domain with a variable fluid depth into a strip of uniform depth (e.g. Fitz-Gerald
279 (1976), Roseau (1976)) was made whereupon the bathymetric variations are projected into a vari-
280 able coefficient in the transformed free surface condition exactly in the form of (54), the only
281 difference being that $F(x)$ in (55) is complex-valued. Porter & Porter (2006) developed their
282 approximation by using an equivalent variational formulation of the boundary-value problem in
283 $x > 0$ and sought approximations to ϕ which are modulated by a depth variation associated with
284 the dominant propagating modes assuming the surface coefficient $F(x)$ is locally constant. The

285 step approximation (see Evans & Linton (1994)) could also be applied here although the recent
 286 work of Porter (2020) has shown the equivalence of ‘mild slope’ methods and step approximations.

287 In $x < 0$, the application of Porter & Porter (2006) is trivial and gives rise to the ordinary
 288 differential equation

$$\eta''(x) + k^2\eta(x) = 0, \quad (56)$$

289 where k now satisfies $k \tanh kh = \omega^2/g$. Since the surface coefficient is constant in $x < 0$ the
 290 propagating modes determined by solutions of (56) are exact.

291 In $x > 0$ the application of the mild slope method results in

$$\eta''(x) + \tilde{k}^2(x)\eta(x) = 0 \quad (57)$$

292 where $\tilde{k}(x) \tanh(\tilde{k}(x)(h_b - \hat{\rho}d)) = F(x)$. Note that (57) results from a simplification made by Porter
 293 & Porter (2006) which neglects a complicated modification to \tilde{k} on the basis of it having a small
 294 effect – for our case the neglected terms are $O(\delta^2)$. The matching conditions are, as before, that

$$\eta(0^+) = \eta(0^-), \quad \eta'(0^+) = \hat{h}^{-1}\eta'(0^-). \quad (58)$$

295 These matching relations arise on account of the variational principle used in Porter & Porter
 296 (2006). It can also be easily verified that the shallow water limit of this mild slope system coincides
 297 with the shallow water model (though only with $B = 0$), in particular $\tilde{k}^2(x) \rightarrow \kappa(x)$ in (46).

298 Solutions of (56) are $\eta(x) = e^{ikx} + Re^{-ikx}$ whilst solutions to (57) are determined by numerical
 299 integration. Specifically, we let

$$\eta(x) = C\eta_1(\hat{x}) + D\eta_2(\hat{x}) \quad (59)$$

300 where $\hat{x} = x/h$ and $\eta_i(x)$ are solutions to (57) in $x > 0$ set by the initial conditions $\eta_1(0) = 1$,
 301 $\eta_1'(x) = 0$ and $\eta_2(0) = 0$, $\eta_2'(x) = 1$. Since $\eta_i(\hat{x})$ will contain both exponentially decaying and
 302 growing solutions but we require $\eta(x) \rightarrow 0$ as $x \rightarrow \infty$ then from (59)

$$D = -C\eta_2(\hat{L})/\eta_1(\hat{L}) \quad (60)$$

303 where $\hat{L} = L/h \gg 1$ is a large numerical truncation parameter representing infinity. That is, large
 304 enough for the constant rate of exponential growth in the solutions to have established itself. From
 305 the behaviour predicted by (48) this should be in excess of $1/(kh)^2$. Numerically we have found
 306 the slightly odd choice $\hat{L} = 50/(kh)^{1.5}$ gives robust and accurate results for the particular numerical
 307 integration routine used (part of the NAG library). Matching the explicit solutions in $x < 0$ to (59)
 308 with (60) via (58) yields

$$R = \frac{\Lambda\eta_2(\hat{L}) - \eta_1(\hat{L})}{\Lambda\eta_2(\hat{L}) + \eta_1(\hat{L})}, \quad \Lambda = \frac{-ikh}{\hat{h}}. \quad (61)$$

309 where $\hat{h} = (h_b - \hat{\rho}d)/h$ as before. The same numerical solution can also be used to numerically
 310 approximate the proportion of incident wave energy absorbed by a device of finite length L . In
 311 $x > L$ we assume the depth returns to h and there exists a transmitted wave $\eta = Te^{ikx}$ propagating
 312 to infinity. For this case the reflection and transmission coefficients are easily found to be solutions
 313 of

$$\begin{pmatrix} \Lambda\eta_2(\hat{L}) + \eta_1(\hat{L}) & -1 \\ \Lambda\eta_2'(\hat{L}) + \eta_1'(\hat{L}) & \Lambda \end{pmatrix} \begin{pmatrix} R \\ T \end{pmatrix} = \begin{pmatrix} \Lambda\eta_2(\hat{L}) - \eta_1(\hat{L}) \\ \Lambda\eta_2'(\hat{L}) - \eta_1'(\hat{L}) \end{pmatrix}. \quad (62)$$

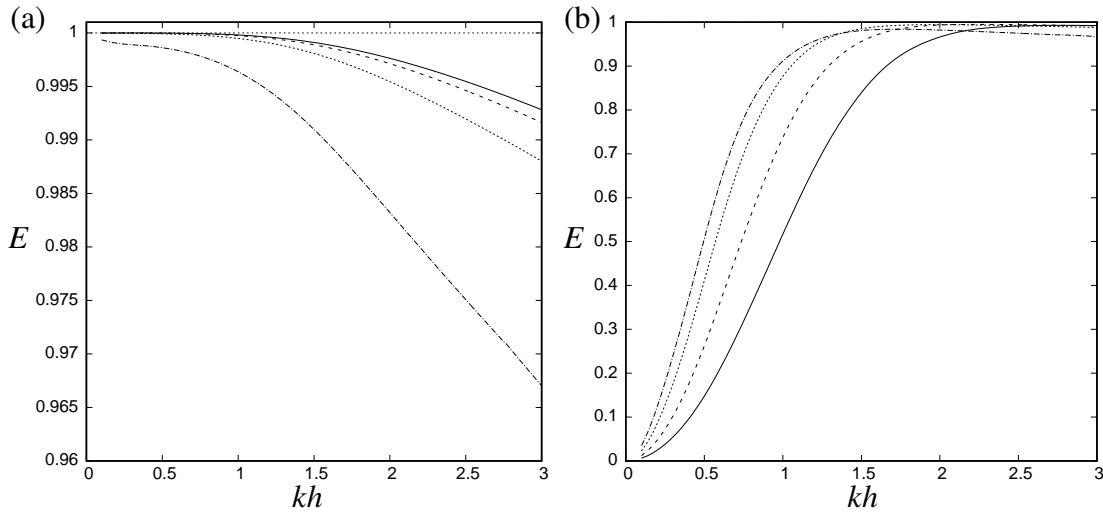


Figure 2. In (a) absorption efficiency against kh for $\delta = 0.025$ (solid), 0.05, 0.1, 0.2 (chained) for a device extending indefinitely into $x > 0$ and in (b) corresponding values for a device of finite length $\hat{L} = 5$.

314 5.2. Results

315 We are interested in the efficiency $E = 1 - |R|^2$ as a function of kh for the semi-infinite absorber
 316 and $E = 1 - |R|^2 - |T|^2$ for the absorber of dimensionless length $\hat{L} = L/h$. Perfect absorption
 317 implies $E = 1$.

318 We have taken $\hat{\rho} = 0.5$ and $d/h = 0.1$ as representative values in the computation of results
 319 using the mild slope approach described in the previous section. In Fig. 2 we show the variation
 320 of E against kh for values of δ between 0.025 and 0.2 assuming an absorber extending indefinitely
 321 into $x > 0$. As $kh \rightarrow 0$, $E \rightarrow 1$ since it is this limit where shallow water theory becomes exact. It
 322 can be seen that the efficiency remains remarkably high across a wide range of wavenumbers with
 323 smaller values of δ – implying a more gradual spatial variation of springs and dampers – giving
 324 the best results.

325 Numerical results have also been produced for an absorber in $x > 0$ with fixed values of
 326 $\hat{\gamma}(x) = 2/(1 - \delta\hat{h})^2$ and $\hat{\sigma}(x) = \delta\hat{h}/(1 - \delta\hat{h})$ and $h = h_b$ implying a sudden jump at $x = 0$ to
 327 the asymptotic values of spring and damper settings taken from the perfectly-absorbing design
 328 and with no adjustment of the depth. We have not displayed these results on any of the figures.
 329 However, we can report that $E \rightarrow 1$ as $kh \rightarrow 0$ though not asymptotically in the manner shown
 330 in Fig. 2(a); instead curves fall rapidly as kh increases to values around $E \approx 0.6$ when $kh = 3$
 331 for all values of δ used in the figures. Thus, we assert that the performance of the perfectly-
 332 absorbing design is a significant improvement upon non-optimised designs having constant spring
 333 and damper settings.

334 In Fig. 3 we hold $\delta = 0.1$ constant and vary the length of the device from $\hat{L} = 2$ up to 16,
 335 confirming that longer devices lead to higher absorption from longer wavelengths.

336 The reader should be reminded that we never set out to optimise the performance of a wave
 337 absorbing device of finite length under $O(kh) = 1$ conditions. Having said that, it is interesting to
 338 note that there are similarities between the curves of efficiency produced here for devices of finite

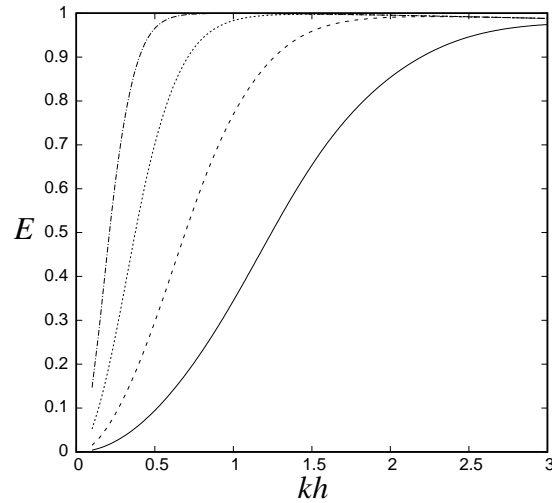


Figure 3. Absorption efficiency against kh for $\delta = 0.1$ and $\hat{L} = 2$ (solid), 4, 8, 16 (chained).

length and curves presented in Haren & Mei (1979) for optimally-designed articulated rafts.

6. Conclusions

We have developed a shallow water model of an array of floating buoys covering the surface to show that all of the energy incident in two-dimensional water waves can be absorbed from waves of all frequencies using spatially-varying spring and damper settings whose tuning is independent of frequency. The approach has relied on what is believed to be a novel variation of the Perfectly Matched Layer (PML) method of Berenger (1994) to perfectly impedance match the shallow water equations for an unloaded free surface to a loaded damped surface.

However, shallow water theory is an approximation for wavenumbers satisfying $kh \ll 1$ where h is the depth and is only exact in the limit $kh \rightarrow 0$. In addition to the proposed wave absorber being semi-infinite in extent implies that the main result is of more theoretical than practical interest.

On the other hand, we have also produced numerical results based on full linear theory to illustrate that perfect absorber design made under shallow water conditions can still absorb most of the available incident energy across a range of wavenumbers.

Appendix: The blockage coefficient

We solve the following problem for a potential $\psi(x, z)$ governed by $\nabla^2 \psi = 0$ in the fluid domain $\{-\infty < x < 0, -1 < z < 0\} \cup \{0 < x < \infty, -h_b/h < z < -\hat{\rho}d/h\}$ with Neumann conditions all boundaries apart from those cutting the flow at the two infinities. As $x \rightarrow -\infty$ we impose $\psi(x, z) \rightarrow x$ and as $x \rightarrow \infty$ we have

$$\psi(x, z) = x/\hat{h} + B \quad (63)$$

where $\hat{h} = (h_b - \hat{\rho}d)/h$. The solution to this problem determines B . The problem is well suited to Schwarz-Christoffel mapping although the boundary in this problem is complicated and we have

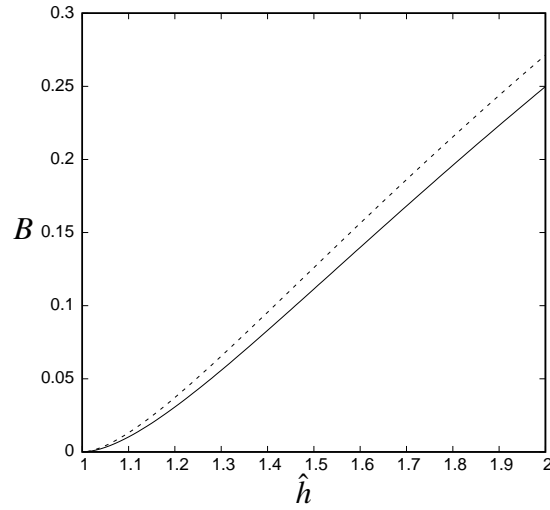


Figure 4. The variation of the blockage coefficient against \hat{h} for $d/h = 0$ using the exact formula (solid) and the crude series approximation (dashed).

360 not attempted to calculate an explicit solution. In the case that $-\hat{\rho}d \approx 0$ the geometry is simplified
 361 and we have from Mei (1983),

$$B = \frac{1}{\pi} \frac{\hat{h}^2 + 1}{\hat{h}} \ln\left(\frac{\hat{h} + 1}{\hat{h} - 1}\right) - \frac{2}{\pi} \ln\left(\frac{4\hat{h}}{\hat{h}^2 - 1}\right) \approx \frac{-(\hat{h} - 1)^2}{\pi} \ln((\hat{h} - 1)/2) \quad (64)$$

362 for $\hat{h} \rightarrow 1^+$.

363 Alternatively, using separation solutions and mode matching to produce an integral equation
 364 for the horizontal flow velocity across $x = 0$ we can easily produce a crude but simple approxima-
 365 tion to B which is

$$B \approx \frac{2}{\pi^3(1 - \hat{\rho}d/h)^2} \sum_{n=1}^{\infty} \left\{ \frac{\sin^2(n\pi\hat{\rho}d/h)}{n^3} + \frac{\hat{h}^2 \sin^2(n\pi(1 - \hat{\rho}d/h)/\hat{h})}{n^3} \right\} \quad (65)$$

366 which will work well for $\hat{\rho}d/h \ll 1$ and $h_b/h \ll 1$. A demonstration is provided by Fig. 4.

367 References

- 368 [1] Berenger, J.-P. A Perfectly Matched Layer for the absorption of electromagnetic waves. *J. Comp. Phys.* 1994:114;185-200.
 369
 370 [2] Cockerell, C., Platts, M. & Comyns-Carr, R. The development of the wavecontouring raft. In: *Proc. Wave Energy Conference. London-Heathrow, H.M.S.O. London, Ed. P. Quarrell. 1978.*
 371
 372 [3] Evans, D.V. A theory for wave-power absorption by oscillating bodies. *J. Fluid Mech.* 1976:77;1-25.
 373 [4] Evans, D.V., Jeffrey, D.C., Salter, S.H. & Taylor, J.R.M. Submerged cylinder wave-energy device: theory and experiment. *Appl. Ocean Res.* 1979:1;3-12.
 374
 375 [5] Evans D.V. & Linton, C.M. On step approximations for water wave problems. *J. Fluid Mech.* 1994:278;229-249.
 376 [6] Fang, J. & Wu, Z. Generalised Perfectly Matched Layer – An extension of Berenger’s Perfectly Matched Layer boundary condition. *IEEE Microwave & Guided Wave Lett.* 1995:5(12);451-453.
 377

- 378 [7] Fitz-Gerald, G.F. The reflexion of plane gravity waves travelling in water of variable depth. *Phil. Trans. R. Soc.*
379 *Lond. A.* 1976:34;49-89.
- 380 [8] Haren, P. & Mei, C.C. Wave power extraction by a train of rafts: hydrodynamic theory and optimum design.
381 *Appl. Ocean Res.* 1979:1(3);147-157.
- 382 [9] Garnaud, X. & Mei, C.C. Wave-power extraction by a compact array of buoys. *J. Fluid Mech.* 2009:635;389-
383 413.
- 384 [10] Mei, C.C. *The Applied Dynamics of Ocean Surface Waves.* Wiley Interscience: New York. 1983.
- 385 [11] Newman, J. Absorption of wave energy by elongated bodies. *Appl. Ocean Res.* 1979:1(4);189–196.
- 386 [12] Porter, R. An extended linear shallow water equation. *J. Fluid Mech.* 2019:876;413-427.
- 387 [13] Porter, R. On the connection between step approximations and depth-averaged models for wave scattering by
388 variable bathymetry. *Q. J. Mech. Appl. Math.* 2020:73(1);84-100.
- 389 [14] Porter, R. & Porter, D. Approximations to water wave scattering by steep topography. *J. Fluid Mech.*
390 2006:562;279-302.
- 391 [15] Roseau, M. *Asymptotic Wave Theory.* North-Holland. 1976.
- 392 [16] Salter, S.H. Wave power. *Nature*, 1974:249;720-724.
- 393 [17] Salter, S., Jeffery, D. & Taylor, J. The architecture of nodding duck wave power generators. *The Naval Architect*
394 1976:1;21-24.
- 395 [18] Stoker, J.J. *Water Waves.* Interscience, New York. 1957.
- 396 [19] Tuck, E.O. Matching problems involving flow through small holes. In *Advances in Applied Mechanics*,
397 1975:15;89-158.
- 398 [20] Weitz, M. & Keller, J.B. Reflection of water waves from floating ice in water of finite depth. *Commun. Pure*
399 *Appl. Maths* 1950:3;581-607.